Dendrochronologia 65 (2021) 125787

Contents lists available at ScienceDirect

Dendrochronologia

journal homepage: www.elsevier.com/locate/dendro

Original article

Micro-site conditions affect Fennoscandian forest growth

Claudia Hartl [a,*], Elisabeth Düthorn [a], Ernesto Tejedor [b], Andreas J. Kirchhefer [c], Mauri Timonen [d], Steffen Holzkämper [e], Ulf Büntgen [f,g,h], Jan Esper [a]

[a] Department of Geography, Johannes Gutenberg University, Mainz, Germany
[b] Department of Atmospheric and Environmental Sciences, University at Albany (SUNY), Albany, New York, USA
[c] Dendroøkologen A.J. Kirchhefer, Tromsø, Norway
[d] Natural Resources Institute Finland, Rovaniemi, Finland
[e] Department of Physical Geography, Stockholm University, Stockholm, Sweden
[f] Department of Geography, University of Cambridge, UK
[g] Swiss Federal Research Institute WSL, Birmensdorf, Switzerland
[h] Global Change Research Centre AS CR, Brno, Czech Republic

ARTICLE INFO

Keywords:
Abiotic site factors
Boreal forest growth
Climate sensitivity
Dendroecology
Scots pine
Tree-ring network

ABSTRACT

The long tradition of dendroclimatological studies in Fennoscandia is fostered by the exceptional longevity and temperature sensitivity of tree growth, as well as the existence of well-preserved subfossil wood in shallow lakes and extent peat bogs. Although some of the world's longest ring width and density-based climate reconstructions have been developed in northern Fennoscandia, it is still unclear if differences in micro-site ecology matter, and if so, whether they have been considered sufficiently in previous studies. We developed a Fennoscandia-wide network of 44 Scots pine ring width chronologies from 22 locations between 59°–70 °N and 16°–31 °E, to assess the effects of moist lakeshores and dry inland micro-sites on tree growth. Our network reveals a strong dependency of pine growth on July temperature, which is also reflected in latitude. Differences in forest productivity between moist and dry micro-sites are likely caused by associated effects on soil temperature. While trees at moist micro-sites at western locations exhibit higher growth rates, this pattern is reversed in the continental eastern part of the network, where increased ring widths are found at drier sites. In addition to the latitudinal increase in growth sensitivity to July temperature, pines at moist sites exhibit an increased dependency of summer warmth. The highest temperature sensitivity and growth coherency, and thus greatest suitability for summer temperature reconstructions, is found in those regions where July mean temperatures range between 11.5 and 13.5 °C, and May precipitation totals do not exceed 100 mm. Our study not only provides guidance for the selection of sampling sites for tree ring-based climate reconstructions, but also reveals the effect of micro-site ecology on Fennoscandian forest growth. The manifestation of micro-site effects varies substantially over the Fennoscandian boreal forest and is predominately triggered by the geographical setting of the stand as expressed by differing abiotic site factors.

1. Introduction

Fennoscandia has a long tradition in dendroclimatological studies (Linderholm et al., 2010), within which different tree-ring parameters were used to reconstruct summer temperatures over the past centuries to millennia (Büntgen et al., 2011, see references herein). Recent efforts include tree-ring stable isotopes to study changes in sunshine duration/cloud cover (Loader et al., 2013; Young et al., 2012), but more commonly the reconstructed climate element is summer season temperature based on tree-ring width or maximum latewood density (e.g., Büntgen et al., 2011; Esper et al., 2012a, b; Esper et al., 2014; Grudd, 2008; Linderholm and Gunnarson, 2005; Linderholm et al., 2014; McCarroll et al., 2013).

In addition to a long academic history and good accessibility, there are at least two more reasons for the high number of tree ring-based climate reconstructions from Fennoscandia: i) a robust temperature signal in tree growth and ii) sample availability over the past centuries to millennia. Concerning the temperature signal, Liebig's law of the minimum, stating that growth is dictated not by the total resources available, but by the scarcest resource (limiting factor), actually reasons

* Corresponding author.
E-mail address: c.hartl@geo.uni-mainz.de (C. Hartl).

https://doi.org/10.1016/j.dendro.2020.125787
Received 16 July 2020; Received in revised form 24 October 2020; Accepted 10 November 2020
Available online 17 November 2020

the suitability of Fennoscandia for such purposes. Many forest sites are near tree-line where cambial activity is mainly limited by growing seasons temperature, a signal that is fingerprinted in tree-ring width. The second requirement of sample availability to build long chronologies is also given in Fennoscandia. Albeit the living trees only cover the past several hundred years in that region, a large number of subfossil wood can be found in lakes there. Due to the anaerobic conditions and short summers with low temperatures, this subfossil wood is very well preserved, over thousands of years (Gunnarson, 2001; Helama et al., 2008), and still suitable for dendrochronological analysis. Samples from subfossil wood can be cross-dated with living trees to produce millennial-length tree-ring chronologies.

It can be assumed that the subfossil wood originally grew in moist conditions at the lakeshore before the trees fell into the lake. For the long chronologies, however, the living tree material was not necessarily sampled at moist lakeshores but at "normal" dry sites (Esper et al., 2012b). As a consequence, the growth conditions and also the limiting factors might vary between the different wood sources, i.e. micro-sites, and potentially influence a climate reconstruction. The living trees are calibrated against the instrumental data, but the derived growth/climate models, might not fully represent the ones of the subfossil wood from moister sites. This micro-site effect issue was already investigated by several regional studies. Some studies found that summer temperature signals were reduced at moist micro-sites compared to dryer sites in many northern Fennoscandian locations (Düthorn et al., 2015, 2016; Linderholm, 2001; Linderholm et al., 2002, 2014; Matskovsky and Helama, 2014), whereas it is the other way around at a location in northern Sweden (Düthorn et al., 2013). Another study by Lange et al. (2018) analysed potential effects at larger spatial scales, from Fennoscandia to Siberia, and found that micro-sites have only minor effects on climate signals, compared to the (changing) local climate regime. It was furthermore discussed if micro-site issues could contribute to the 'divergence problem' (Wilmking et al., 2005), i.e. the loss of trees' temperature sensitivity since the mid-20th century (D'Arrigo et al., 2008; Esper and Frank, 2009 for an overview). Based on the inconsistency of micro-site effects as well as the reduced climate sensitivity during recent decades, the a priori suitability of trees from Fennoscandia for temperature reconstructions was questioned (Düthorn et al., 2015; Edvardsson et al., 2015; Hellmann et al., 2016; Lange et al., 2018; Linderholm et al., 2014; Wilmking et al., 2020).

All of the above-mentioned studies investigated micro-site effects at a maximum of six locations and results among these studies were contradicting. It is therefore not entirely clear, how micro-site effects are manifested considering a wider ecological amplitude, what exactly influences the presence and strength of such effects, and if these are a possible cause of the divergence problem. To address these issues, we compiled a network of 44 micro-site chronologies from 22 locations, covering several ecological gradients throughout Fennoscandia, and analysed these data to identify potentially differing growth responses. We first assess (dis)similarities among micro-site chronologies within the entire network, then evaluate the varying growth rates and climate signals and their stability over time, and relate these findings to varying abiotic factors throughout the network to understand and explain growth and climate response changes among micro-sites in time and space. This approach allows us to place the new pine tree-ring width network into a wider context of Fennoscandian boreal forest growth.

2. Material and methods

2.1. Tree-ring network

We developed a tree-ring width micro-site network in Fennoscandia that comprises 1983 Scots pine (*Pinus sylvestris* L.) trees from 22 sampling locations along a north-south gradient of ~1200 km and a west-east gradient of ~700 km between 59° and 70 °N and 16° and 31 °E (Fig. 1). At each location, we sampled trees growing at moist sites

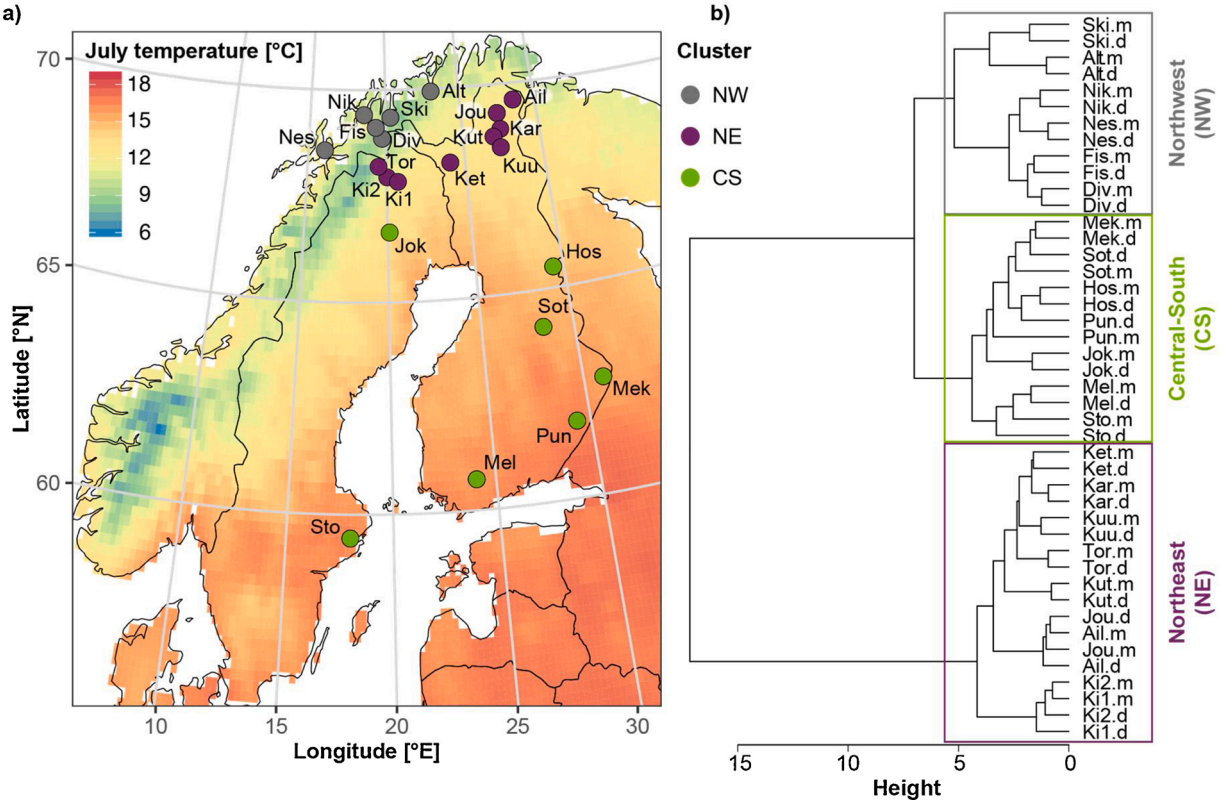

Fig. 1. a) Network of 44 tree-ring width micro-sites across Fennoscandia, and superimposed on July temperature means based on instrumental measurements from the 1961-1990 period. b) Hierarchical cluster analysis of the 44 micro-site chronologies calculated over the 1903-2006 common period.

directly at the lakeshore (data denoted as Xyz.m) and at locally drier sites several meters inland (Xyz.d) during several field campaigns between 2012 and 2016. We collected two 5 mm diameter increment cores per tree at breast height (~1.30 m), and a minimum of 30 healthy looking trees with heterogenous dominance and age structure were sampled at each micro-site. This dataset is supplemented by existing data from five locations following the same sampling design (Ki1, Ki2, Ket, Sto, Tor; Büntgen et al., 2011; Esper et al., 2012b; Düthorn et al., 2013) (Table 1). A total of 3965 ring-width series finally allows placing the new 44 micro-site chronologies into a wider context of Fennoscandian boreal forest growth. Tree-ring width was measured at 0.01 mm resolution using LINTAB measurement devices and the TSAPWin software (both Rinntech, Heidelberg, Germany). Cross-dating was verified visually and statistically using the program COFECHA (Holmes, 1983).

Fig. 1 a) Network of 44 tree-ring width micro-sites across Fennoscandia, and superimposed on July temperature means based on instrumental measurements from the 1961–1990 period. b) Hierarchical cluster analysis of the 44 micro-site chronologies calculated over the 1903–2006 common period.

2.2. Chronology development

To remove age-related growth trends, we produced dimensionless ring-width indices (RWI) by detrending the raw ring-width series individually using cubic smoothing splines with a 50% frequency cut-off at 100 years (Cook and Peters, 1981). Micro-site chronologies were constructed by averaging the detrended single series using a robust mean (Mosteller and Tukey, 1977). Inter-series correlation (rbar), i.e. the average Pearson's correlation coefficient among all detrended single series within a micro-site, is used to estimate chronology covariance (Table 1). Additional descriptive statistics include the mean series length (MSL), representing an estimate of mean tree age within a micro-site chronology, average growth rate of raw ring-width data (AGR_{all}), representing the mean ring-width of the overall micro-site stand, and first order autocorrelation (Lag-1) of detrended data as presented in Table 1.

2.3. Chronology (dis-)similarities

Inter-site comparisons were performed using two different techniques: to identify dissimilarities within the micro-site network, a hierarchical cluster analysis (HCA) was performed, employing the Ward's method and using the Euclidean distance as distance measure. To estimate covariance within the network, we calculated Pearson's correlation coefficient among the micro-site chronologies. Considering the grouping of the HCA we calculated average inter-chronology correlations ($rbar_C$) for the dry ($rbar_{Cd}$), moist ($rbar_{Cm}$) and entire ($rbar_{Call}$) micro-site chronologies. All these analyses were performed over the common 1903–2006 period of chronology overlap (though one single chronology Kuu.m is shorter; Table 1).

2.4. Growth assessment

The growth behaviour at different micro-sites was described by AGR_{all} calculated over the overall tree age. We additionally calculated the mean growth over the first 40 years of tree age (AGR_{C40}), to mitigate the influence of tree age on AGR_{all}. Based on that, we calculated the difference of the dry and moist micro-sites $\Delta AGR_{C40} = AGR_{C40.d} - AGR_{C40.m}$ at each location and across the network. To evaluate potential dependencies of AGR and ΔAGR on abiotic factors including latitude, longitude, elevation, July temperature and May precipitation (E-OBS v19.0, Cornes et al., 2018), we used generalized additive models (GAM) with a penalized thin plate regression spline as spline base for each factor separately (Wood, 2017).

Table 1
Chronology characteristics of the Fennoscandian tree-ring width micro-site network. MSL = mean series length, AGR_{all} = average growth rate, Rbar = inter-series correlation, Lag-1 = first order autocorrelation.

Site	Cluster	Latitude [°N]	Longitude [°E]	Elevation [m asl]	Period		MSL [a] ± SD		AGR_{all} [mm] ± SD		Rbar*		Lag-1*		Number	
					Dry	Moist	Dry	Moist	Dry	Moist	Dry	Moist	Dry	Moist	Dry	Moist
Ail	NE	69.52	28.57	120	1733–2011	1802–2011	172 ± 83	111 ± 73	0.58 ± 0.29	0.59 ± 0.24	0.43	0.32	0.72	0.65	80	110
Alt	NW	69.92	23.11	73	1812–2015	1837–2015	128 ± 43	95 ± 55	0.86 ± 0.24	0.93 ± 0.42	0.36	0.3	0.76	0.69	93	73
Div	NW	68.86	19.59	320	1817–2013	1808–2013	86 ± 65	74 ± 61	1.01 ± 0.44	1.07 ± 0.46	0.23	0.25	0.66	0.66	105	77
Fis	NW	69.06	19.34	151	1797–2014	1758–2014	83 ± 70	97 ± 76	0.78 ± 0.35	0.79 ± 0.39	0.29	0.2	0.61	0.7	72	67
Hos	CS	65.49	29.4	229	1766–2011	1763–2011	120 ± 70	97 ± 66	0.66 ± 0.29	0.65 ± 0.28	0.38	0.29	0.73	0.75	101	99
Jok	CS	66.65	20.11	302	1750–2013	1763–2013	87 ± 73	102 ± 86	0.82 ± 0.24	0.89 ± 0.34	0.41	0.27	0.6	0.66	126	86
Jou	NE	69.26	27.4	200	1708–2011	1737–2011	136 ± 96	95 ± 81	1.01 ± 0.52	0.73 ± 0.33	0.31	0.27	0.74	0.63	170	144
Kar	NE	68.83	27.31	258	1708–2011	1556–2011	142 ± 87	215 ± 114	0.68 ± 0.25	0.43 ± 0.16	0.28	0.35	0.68	0.73	74	126
Ket	NE	68.22	24.05	300	1749–2006	1762–2006	143 ± 87	169 ± 79	0.52 ± 0.16	0.6 ± 0.21	0.27	0.43	0.73	0.78	66	49
Ki1	NE	67.9	20.1	451	1826–2009	1816–2009	77 ± 50	83 ± 59	1.06 ± 0.34	0.92 ± 0.28	0.39	0.38	0.79	0.69	60	68
Ki2	NE	67.95	20.03	430	1781–2006	1793–2006	106 ± 81	85 ± 80	0.77 ± 0.22	0.92 ± 0.42	0.35	0.37	0.7	0.61	104	87
Kut	NE	68.77	27.15	170	1772–2015	1762–2015	144 ± 54	136 ± 64	0.7 ± 0.19	0.68 ± 0.20	0.48	0.43	0.85	0.81	80	73
Kuu	NE	68.45	27.36	302	1856–2011	1931–2011	50 ± 48	55 ± 27	1.3 ± 0.49	1.04 ± 0.45	0.18	0.28	0.61	0.62	87	88
Mek	CS	62.73	31.01	147	1903–2011	1849–2011	62 ± 29	83 ± 41	1.39 ± 0.66	0.88 ± 0.36	0.23	0.26	0.74	0.71	125	88
Mel	CS	60.73	24.06	120	1891–2011	1899–2011	87 ± 30	80 ± 21	1.17 ± 0.34	1.26 ± 0.32	0.29	0.28	0.63	0.68	116	93
Nes	NW	68.57	16.06	345	1759–2013	1795–2013	90 ± 78	69 ± 60	0.98 ± 0.46	1.32 ± 0.52	0.23	0.22	0.53	0.52	71	93
Nik	NW	69.36	18.73	90	1845–2014	1878–2014	76 ± 60	74 ± 40	0.8 ± 0.27	0.86 ± 0.37	0.34	0.29	0.67	0.72	69	63
Pun	CS	61.81	29.31	78	1838–2011	1875–2011	101 ± 40	80 ± 28	1.31 ± 0.37	1.15 ± 0.44	0.37	0.43	0.81	0.75	102	84
Ski	NW	69.35	20.32	72	1823–2013	1836–2013	92 ± 54	76 ± 36	0.46 ± 0.16	0.62 ± 0.27	0.29	0.22	0.7	0.8	104	98
Sot	CS	64.12	28.34	148	1881–2011	1880–2011	93 ± 38	56 ± 40	0.91 ± 0.36	0.9 ± 0.32	0.26	0.16	0.77	0.64	93	98
Sto	CS	59.44	17.99	20	1854–2009	1812–2009	93 ± 53	120 ± 54	1.22 ± 0.50	1.26 ± 0.40	0.38	0.26	0.57	0.67	58	69
Tor	NE	68.2	19.8	390	1810–2006	1819–2006	89 ± 74	59 ± 59	0.95 ± 0.40	1.24 ± 0.48	0.35	0.27	0.67	0.6	97	79

2.5. Climate signals

Growth/climate response analyses were performed using the detrended micro-site chronologies and monthly mean temperature and precipitation sums. Climate data representative of each site were obtained from E-OBS v19.0 gridded data set (0.25°x0.25° grid, Cornes et al., 2018). Bootstrapped correlations for previous year June to current year September climate data were calculated over the 1950–2006 common period. To identify which micro-site has a higher climate signal at each location, we calculated residuals between the dry micro-site correlations and the moist micro-site correlations ($\Delta r_l = r_{dry} - r_{moist}$). The dependence of July temperature signals inherent to the chronologies to abiotic factors was again checked using GAMs. Changes of July temperature signals over time were examined using 25-year moving correlations and a split period approach over the 1950–1978 and 1979–2006 periods. To analyse the actual difference of the temperature response change over time we calculated $\Delta r_t = r_{1950–1978} - r_{1979–2006}$. All statistical procedures were performed using R 3.5.3 (R Core Team, 2019) and the packages dplR (Bunn et al., 2012), mgcv (Wood, 2017), and treeclim (Zang and Biondi, 2015).

3. Results

3.1. Network characteristics and chronology (dis-)similarities

The Fennoscandian micro-site network can be subdivided into three main groups based on the HCA: northwestern Norway (NW), north-eastern Fennoscandia (NE) and central-south Fennoscandia (CS) (Fig. 1). The NW cluster includes six locations from coastal regions in the luv of the Scandes. The NE cluster comprises nine locations in the lee of the Scandes, in Sweden and Finland, all north of the polar circle. The remaining seven locations of the CS cluster are, except of one location (Jok), all situated south of the Arctic Circle. Within a cluster, the micro-site chronologies from one location are not necessarily statistically

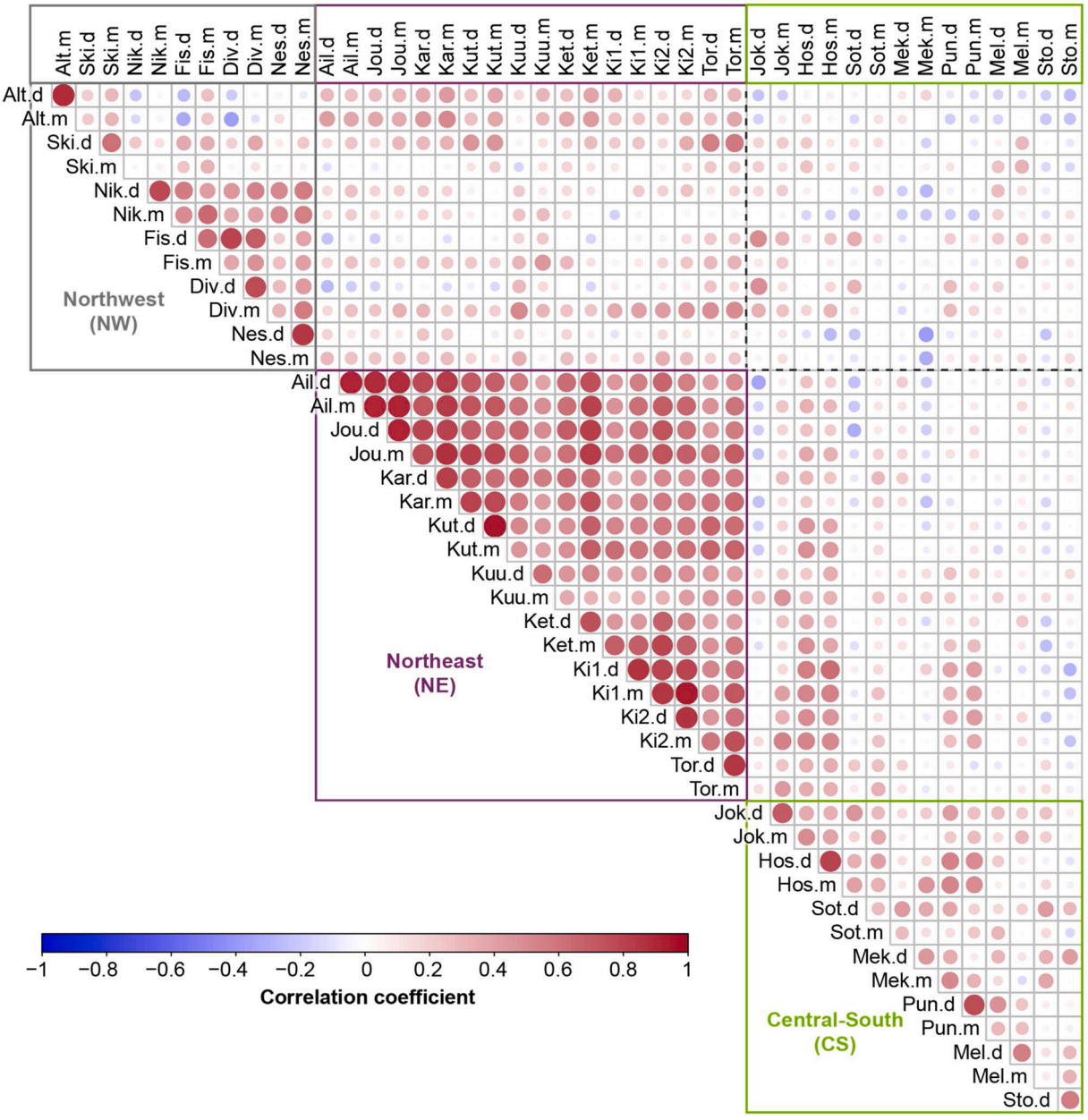

Fig. 2. Pearson's cross-correlation coefficients (as represented by colour and circle size) between all 44 Fennoscandian micro-site chronologies calculated over the 1903-2006 common period (though Kuu.m is shorter).

closer to each other than to a micro-site chronology from another location (Fig. 1b), except for the NW cluster, where highest similarities are recorded between the moist and dry chronologies of one location. In contrast, in the NE cluster, for example, Ki1.m and Ki2.m are more similar compared to their dry counterpart. However, the dissimilarity of associated micro-site chronologies at one location is generally not high as can be derived in Fig. 1b.

The correlation matrix (Fig. 2) underlines and refines the results of the HCA, albeit it also shows the general inconsistence of the year-to-year variability when considering the overall network. For instance, the northernmost chronologies from Alt are anticorrelated with the southernmost chronologies from Sto ($r \approx -0.2$).

Fig. 2 Pearson's cross-correlation coefficients (as represented by colour and circle size) between all 44 Fennoscandian micro-site chronologies calculated over the 1903–2006 common period (though Kuu.m is shorter).

The highest covariances are found among the NE cluster chronologies showing correlation coefficients of $r \geq 0.4$ considering all chronologies. Only the chronologies from Kuu show lower coherence (minimum $r = 0.25$) with the other chronologies from that cluster. Within the NW cluster, the picture is quite different, as there is a larger range between closely correlated and even anti-correlated chronologies (e.g. Alt at the northern coastline with r up to –0.37 with inland chronologies Fis and Div). In the CS cluster we find no consistent covariance among the chronologies with a wide range of r values.

The moist-to-dry correlation is generally higher in the NE cluster, ranging between $r = 0.76$ (Ket) to 0.95 (Kut) and is only low for Kuu ($r = 0.63$) but this might be connected to the shorter period considered as Kuu.m only goes back until 1931. With r values between 0.62 and 0.88 the within location correlation is also high in the NW cluster. The lowest correlation coefficients between moist-to-dry chronologies are found in the CS cluster ranging between 0.29 (Sto) and 0.8 (Hos).

By plotting all chronologies according to their corresponding cluster (Fig. 3), the afore mentioned results get obvious also visually. The chronologies within the NE cluster have a very high synchronicity which is also reflected in high $rbar_C$ values, albeit the covariance is highest when combining all dry ($rbar_{Cd} = 0.76$) chronologies. It is still high within the moist ($rbar_{Cm} = 0.73$) or when considering all chronologies ($rbar_{Call} = 0.75$), but the covariance of the cluster mean dry and moist chronology is with $r_{m/d} = 0.97$ extremely high. In the NW cluster the covariance visually seems relatively high, only the Alt chronologies stick out in the 1940s due to artificial smoke pollution in the Second World War (Hartl et al., 2019). However, the $rbar_C$ values are much lower compared to the NE cluster and highest covariance is found within the moist chronologies ($rbar_{Cd} = 0.27$, $rbar_{Cm} = 0.36$, $rbar_{Call} = 0.35$). The moist and dry cluster means correlate with only $r_{m/d} = 0.84$. The CS cluster seems noisy also visually and the $rbar_C$ values are even lower than in the NW cluster, but here highest covariance is found among the dry chronologies ($rbar_{Cd} = 0.32$, $rbar_{Cm} = 0.25$, $rbar_{Call} = 0.31$, $r_{m/d} = 0.81$).

Fig. 3 All 44 micro-site chronologies plotted within their respective cluster. Semi-transparent red/blue colours represent the single dry/moist micro-site chronologies in the NW cluster (upper panel), NE cluster (middle) and CS cluster (lower panel) and bold lines indicate the respective cluster means. Chronologies were truncated at a minimum replication of five series and rbar values refer to the 1903–2006 common period.

3.2. Growth behaviour

The dependency of growth characteristics to abiotic factors was analysed via the AGR_{all} of the entire period, i.e. the mean growth of the entire stand (Fig. 4a), as well as the stand-level growth over cambial ages 1–41 (AGR_{C40}) (Fig. 4b and c) but only a limited number of factors explain the variance of growth rates significantly. AGR_{all} is strongly dependent on the MSL, with the GAM explaining 34% of the variance, and there is no difference in the moist or dry micro-sites as well as the shape of the models are very similar (Fig. 4a). Latitude appears to be an important factor, particularly in the CS cluster, whereas longitude and elevation are unimportant for differences in AGR_{all}. In contrast, July temperatures significantly trigger AGR_{all} but this also Fig. 4 Growth rates as a function of mean series length (MSL) and different abiotic site factors. a) Average growth rate (AGR_{all}), representing the mean ring-width of the overall stand, b) AGR_{C40} represent the mean growth for the first 40 years of tree age, and c) the difference of the dry and moist micro-site AGR_{C40} ($\Delta AGR_{C40} = AGR_{C40.d} - AGR_{C40.m}$).

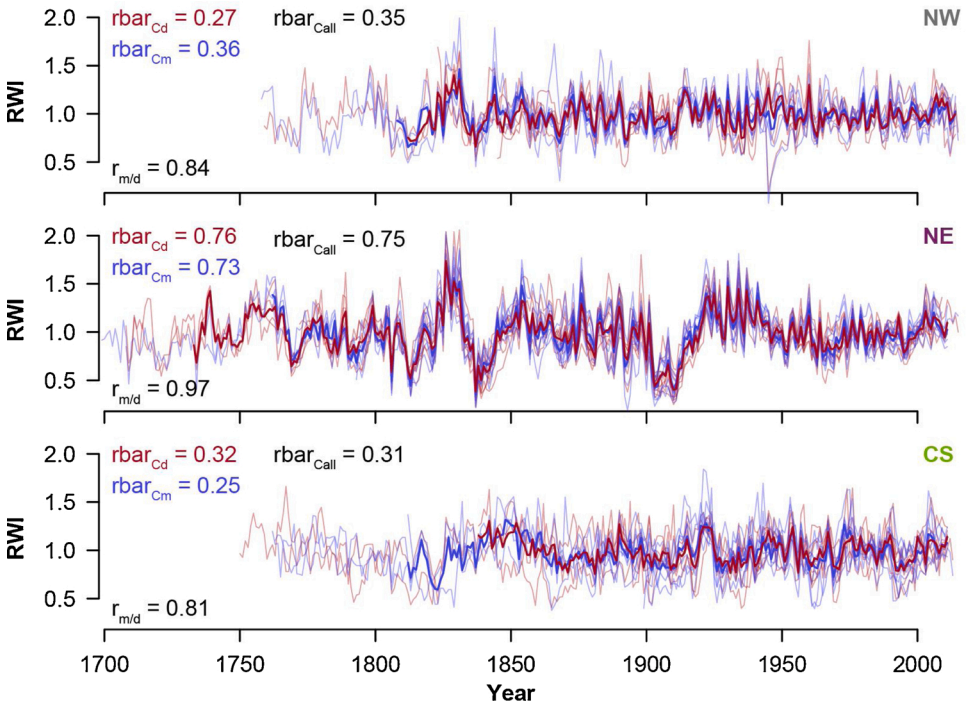

Fig. 3. All 44 micro-site chronologies plotted within their respective cluster. Semi-transparent red/blue colours represent the single dry/moist micro-site chronologies in the NW cluster (upper panel), NE cluster (middle) and CS cluster (lower panel) and bold lines indicate the respective cluster means. Chronologies were truncated at a minimum replication of five series and rbar values refer to the 1903-2006 common period. (For interpretation of the references to colour in this figure legend, the reader is referred to the web version of this article).

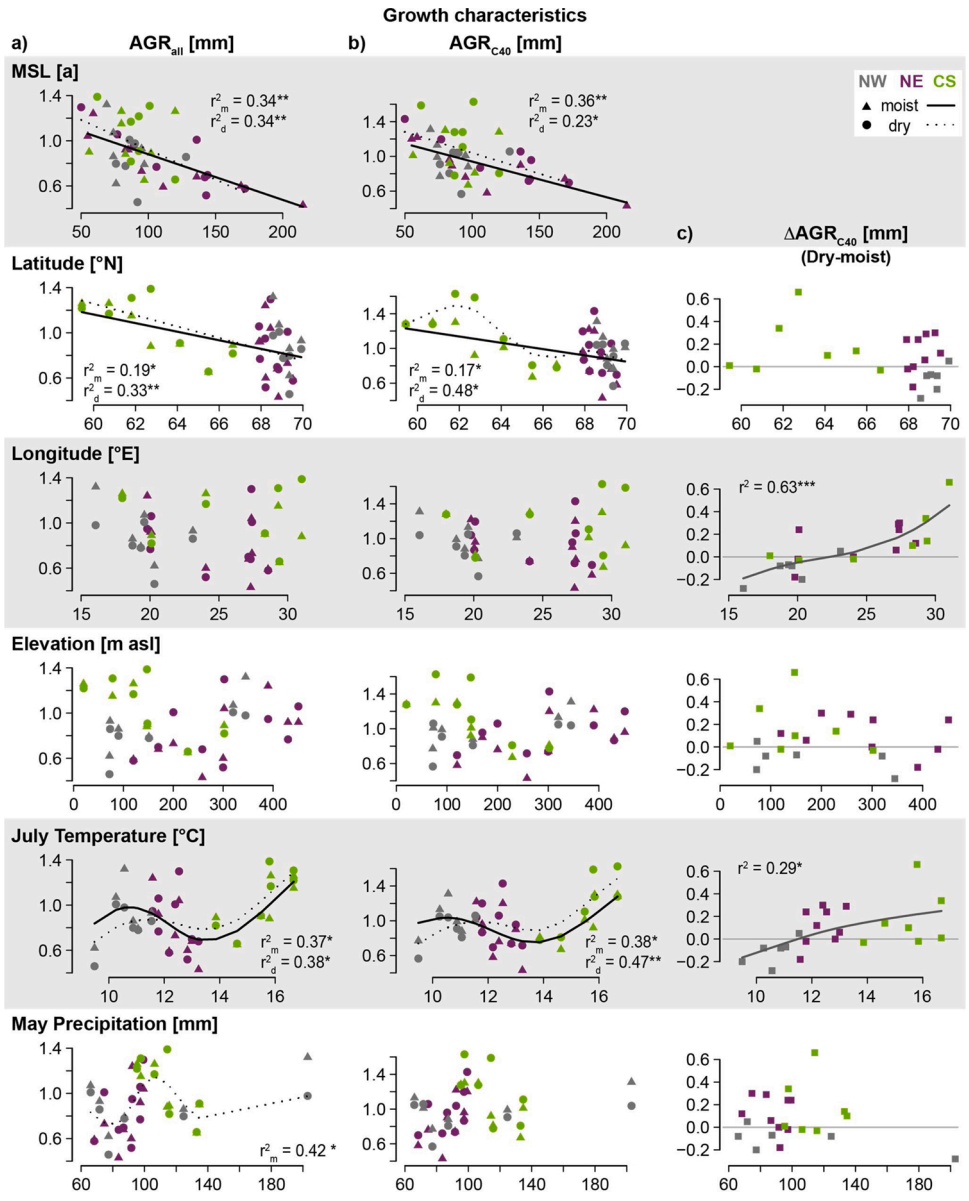

Fig. 4. Growth rates as a function of mean series length (MSL) and different abiotic site factors. a) Average growth rate (AGR_{all}), representing the mean ring-width of the overall stand, b) AGR_{C40} represent the mean growth for the first 40 years of tree age, and c) the difference of the dry and moist micro-site AGR_{C40} ($\Delta AGR_{C40} = AGR_{C40.d} - AGR_{C40.m}$).

shows the distribution of the micro-site network along a temperature gradient. In the NW cluster, trees reach higher growth rates with increasing temperatures. This pattern differs from the NE cluster, where we can actually see a downwards trend of growth rates with increasing temperatures. Within the CS cluster, higher growth rates are found again at sites with higher temperatures. The GAM explains 37% (38%) of the variance for the moist (dry) micro-sites and also the shape of the models is similar, albeit the slopes are steeper for the moist micro-sites. For May precipitation, there are differences among the clusters; with increasing May precipitation, trees grow faster in the NE cluster, whereas that trend is inverted for the CS cluster. In the NW cluster, AGR_{all} seems independent from precipitation sums. The GAM only significantly explains the variance of AGR_{all} for the moist micro-sites (42%).

We considered the AGR_{C40} for cambial age 1–41 years for our analyses (Fig. 4b) as we found the most pronounced differences in the moist and dry sites for that tree ages for all locations (see Fig. S1). Even though the age aligned AGR_{C40} should be less sensitive to MSL, i.e. tree age, 23% (36%) of the variance can be explained by the MSL for the dry (moist) sites. In general, we find the same dependencies or independencies of all abiotic factors as for AGR_{all} as described above, albeit the explained variance by the GAMs slightly vary (see Fig. 4a and 4b). However, to analyse the differences between the growth behaviour of dry and moist micro-sites (ΔAGR_{C40}) it is more robust to focus on cambial age aligned AGR_{C40}s (Fig. 4c). Overall, we find at eleven locations higher growth rates at the dry micro-site, at five locations there is almost no difference and at six locations, the moist micro-sites have higher growth with a cambial age up to 41 years. Latitude, elevation and May precipitation seem irrelevant to explain growth differences between the micro-sites. In contrast, longitude explains 63% of the variance with locations in the West having higher growth rates at the moist micro-sites but locations in the East having higher growth rates at the dry micro-sites, independent of the cluster. The July temperature is revealed as an important factor. At locations with temperatures below 11.5 °C, which pretty much represents the NW cluster, we find higher growth rates at the moist micro-site (except for one location). Above that temperature and for the NE and CS cluster we rather find higher growth rates at the

dry micro-sites. The GAM explains 29% of that pattern. Plotting these results in space (Fig. 5a) highlights that at the coastal and western locations the wet micro-sites have higher growth rates compared to the eastern and warmer location, where the dry micro-sites show higher growth-rates.

Fig. 5 Spatial pattern of the differences between dry and moist micro-sites. a) Difference of the average growth rate in the juvenile phase (cambial age 1–41, dry – moist), with red colours indicating higher growth rates at the dry micro-site, grey colours indicating almost no difference and blue colours higher growth rates at the moist micro-site. b) Differences of the July temperature response (dry – moist), with red colours indicating higher temperature signals at the dry micro-site, grey colours indicating almost no difference and blue colours higher temperature signals at the moist micro-site.

3.3. Climate response

Monthly growth/climate response patterns reveal different climate sensitivities of the individual locations (Fig. S2). However, among the whole network, July is the most frequent month showing significant correlations for temperature (31 out of 44 cases), and May for precipitation (15 cases). As temperature is more important for tree growth in Fennoscandia, we focus on the temperature response patterns in the further analyses.

Overall, the July temperature signal varies among the micro-site network and these variations can partly be explained by abiotic factors. Plotting the July temperature response against abiotic factors demonstrates that the signal does not increase linearly with latitude (Fig. 6a). The correlations increase with latitude, reaching highest values at ~68 °N, but the GAM indicates signal weakening further north, which is most pronounced at the moist micro-sites. Longitude has no significant effect when considering the entire network, though this factor seems to be important in the CS cluster showing increasing correlations with increasing longitude. For the moist micro-sites, elevation seems to explain some variance of the correlation coefficients, but the slope of the model is rather flat, and the factor appears less important within the NE cluster. The absolute July temperature is the most significant factor for the July temperature signal inherent to tree-ring width. However, similar to latitude, this relationship is not linear but strongest in the temperature range of the NE cluster (~12 °C to 13.5 °C, see purple colours in Fig. 6a). Finally, there is no significant relationship between May precipitation and July temperature response, although we find strongest temperature signals at May precipitation sums < 100 mm, at least in the NE and NW clusters.

Regarding response differences between moist and dry micro-sites (Fig. 5b and 6b), the only striking feature is a stronger July temperature signal at the moist micro-site for 18 locations. At only 4 locations of the network, the dry micro-site shows a higher response, though without any dependence on region/cluster. None of the abiotic factors can explain these differences and there seems to be no systematic pattern among the clusters.

Running (Fig. S3) and split-period correlations (1950–1978 and 1979–2006) reveal a frequent decrease of signal strength (as expressed by positive Δr_t values; Fig. 6c) at the moist micro-sites, compared to the dry sites. Eleven dry micro-sites and only five moist micro-sites show higher temperature sensitivity in the later period (i.e. negative Δr_t values). Thereby, five dry Fig. 6 July temperature response patterns of the micro-site network as a function of different abiotic site factors. a) Correlation coefficient of the micro-site chronologies with July temperature over the 1950–2006 period. Filled symbols indicate significant correlations at $p < 0.05$. b) Difference of the July temperature response correlation coefficient between the dry and moist micro-site ($\Delta r_l = r_{dry} - r_{moist}$) as shown in a). c) July temperature response change over time at each micro-site ($\Delta r_t = r_{1950–1978} - r_{1979–2006}$).

micro-sites and three moist micro-sites show a substantial increase ($\Delta r_t < -0.16$), whereas three dry micro-sites and five moist micro-sites

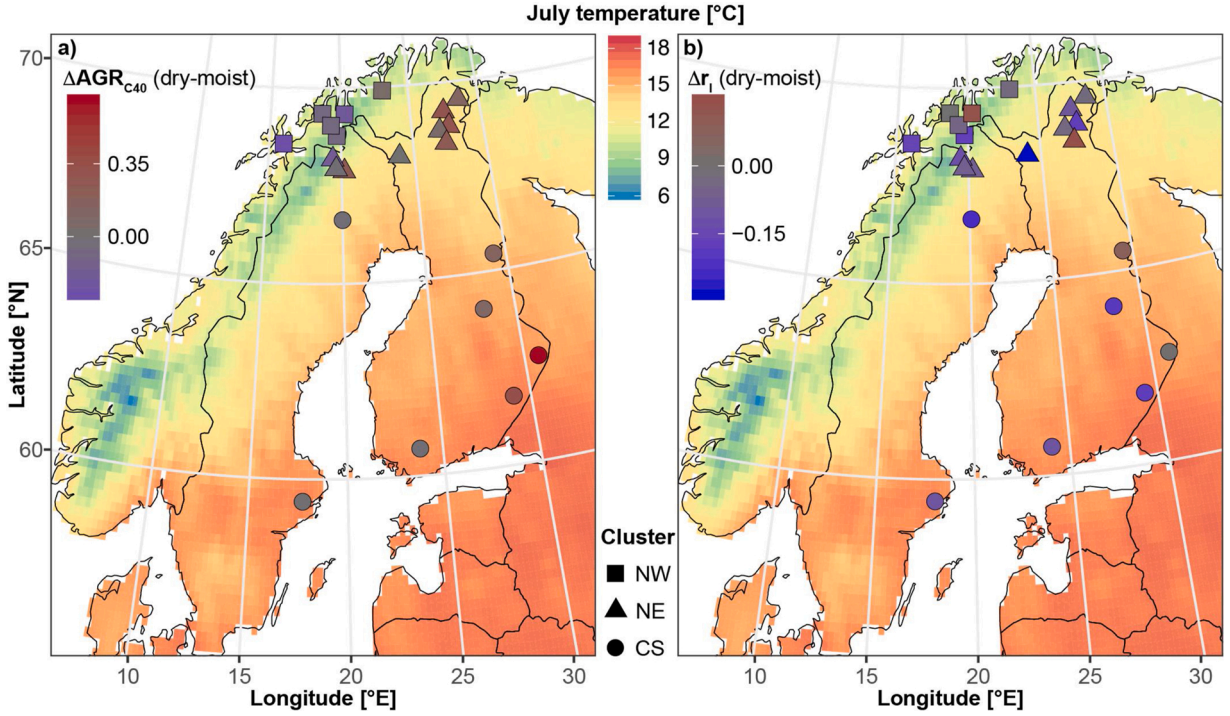

Fig. 5. Spatial pattern of the differences between dry and moist micro-sites. a) Difference of the average growth rate in the juvenile phase (cambial age 1–41, dry – moist), with red colours indicating higher growth rates at the dry micro-site, grey colours indicating almost no difference and blue colours higher growth rates at the moist micro-site. b) Differences of the July temperature response (dry – moist), with red colours indicating higher temperature signals at the dry micro-site, grey colours indicating almost no difference and blue colours higher temperature signals at the moist micro-site. (For interpretation of the references to colour in this figure legend, the reader is referred to the web version of this article).

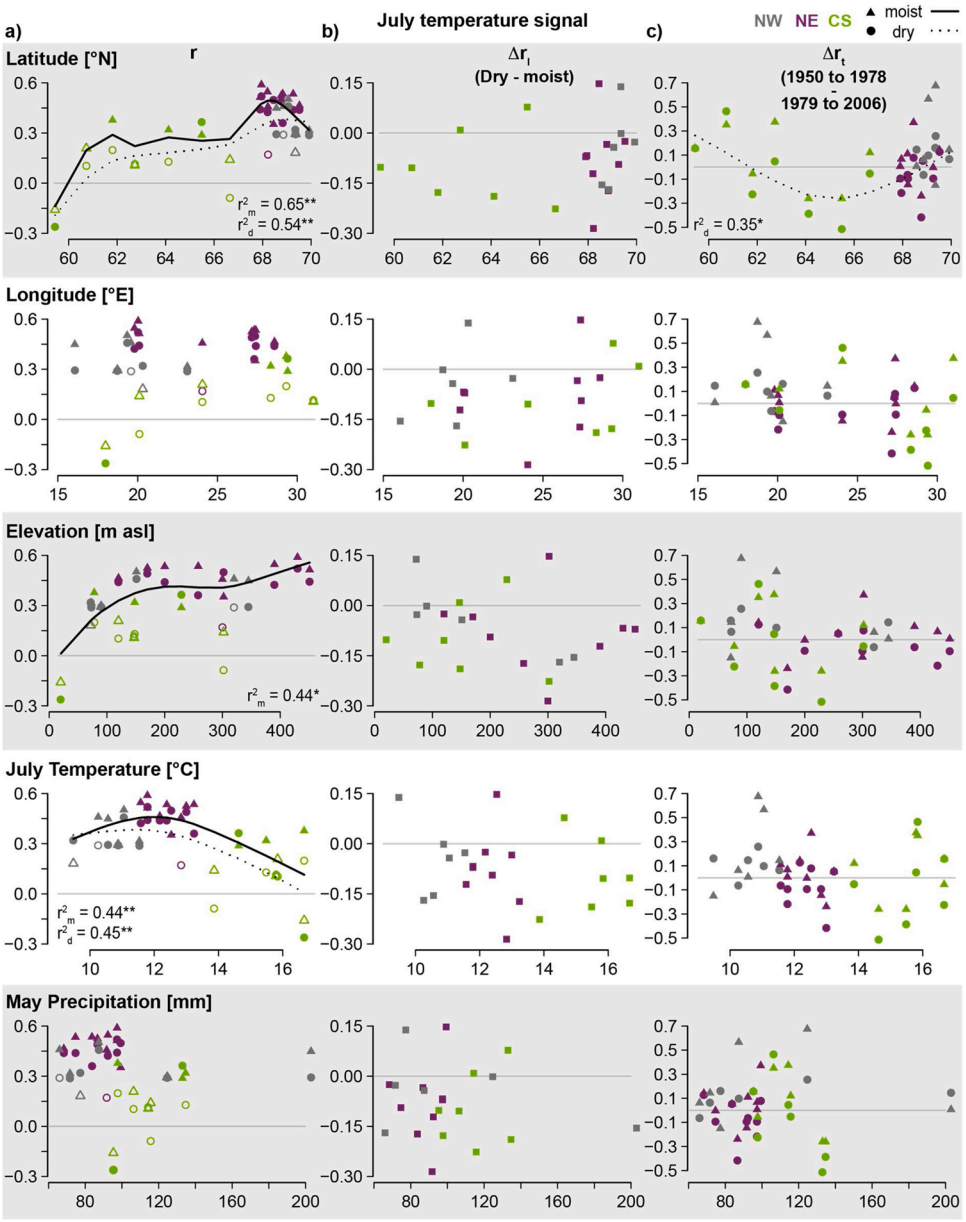

Fig. 6. July temperature response patterns of the micro-site network as a function of different abiotic site factors. a) Correlation coefficient of the micro-site chronologies with July temperature over the 1950-2006 period. Filled symbols indicate significant correlations at $p < 0.05$. b) Difference of the July temperature response correlation coefficient between the dry and moist micro-site ($\Delta r_l = r_{dry} - r_{moist}$) as shown in a). c) July temperature response change over time at each micro-site ($\Delta r_t = r_{1950\text{-}1978} - r_{1979\text{-}2006}$).

show a substantial decrease ($\Delta r_t > 0.16$) of the temperature sensitivity. This distribution of signal gains or losses cannot be explained significantly by any of the analysed abiotic factors except for the dry pattern and latitude.

4. Discussion

There are still uncertainties about micro-site effects in dendroclimatology (Düthorn et al., 2013, 2015, 2016; Lange et al., 2018; Linderholm, 2001; Linderholm et al., 2002, 2014; Matskovsky and Helama, 2014). Yet, no general conclusions could be drawn because only a limited number of sites were analysed. Here we try to resolve this issue across Fennoscandia and analysed 22 locations covering wide ecological gradients.

4.1. Network characteristics: geographical region overrides micro-site differences

The cluster analysis divides the 44 micro-site chronologies in three groups. Thereby the geographical region seems to override the micro-site differences, as in most cases the corresponding micro-sites are statistically closer to each other than to other locations (Fig. 1). This is underlined by the high correlation coefficients that do not recede 0.63 in the NW and NE cluster and 0.55 in the CS cluster except for two locations (Sot and Mek) (Fig. 2). The high correlation coefficients and synchronicity among all chronologies within the NE cluster (see Figs. 2 and 3) suggests that tree growth is controlled by an exclusive and trans-regional limiting factor at these locations even though there is a maximum distance of 440 km (Tor in the West and Ail in the East) between some locations. In the CS and NW clusters it seems that the limiting factors among the locations vary, leading to lower correlation coefficients as well as lower rbar values among chronologies. This is not fully unexpected though, as the locations in the CS cluster are distributed over an even larger region exceeding 800 km between single locations. The differences of site factors over these distances are stronger, as for example daylength or irradiance in these latitudes. The locations of the NW cluster are all situated in a fjord landscape indicating that the relief strongly influences the micro-climatic conditions.

4.2. Controlling factors for boreal forest growth on trans-regional and micro-site scale

The assessment of growth rates showed that bulk cambial activity is mostly controlled by latitude and temperature in Fennoscandia, regardless of the micro-site (Fig. 4). Mean ring-widths decreases with increasing latitude, as tree-line is getting closer (Hartl-Meier et al., 2014; Körner, 2012; Paulsen et al., 2000). The dependence of growth rates on July temperature, however, differs among the clusters. While higher temperatures lead to higher growth rates in the NW and CS cluster, this effect is reversed in the NE cluster. This might be connected to the water availability as we also found a dependence of growth rates to May precipitation in the NE cluster indicating that trees can only benefit from higher temperatures if there is also enough water available in spring.

The growth rate differences between moist and dry micro-sites are linked to longitude and July temperatures (Fig. 4c and 5a). In the study region, these factors are controlled by the North Atlantic Current (the extension of the Gulf Stream in Northern Europe), which is decreasing from West to East and strongly influences temperature conditions during all seasons. Generally, we found that in the NW cluster trees from the moist micro-site grow faster, whereas in the NE and CS cluster the dry micro-site trees showed higher growth rates. In the coastal western region (and luv of the Scandes), the winter and spring temperatures are much milder, compared to the eastern more continental region (lee of the Scandes), leading to less soil frost. If the soil is not frozen, trees do have immediate access to water at the beginning of the growing season, which is likely particular beneficial for trees from moist micro-sites compared to the dry micro-sites. In the eastern area, i.e. CS and NE clusters, soil frost might persist longer at the beginning of the growing season so that there is no advantage of better water availability at these sites. In contrast, soils are thawed earlier at the dry micro-sites so that tree growth can start earlier in the year and the growing season is hence longer.

4.3. Effects of micro-site specific growth rates on chronology development and climate signals

Besides an ecological explanation, growth rate differences are first and foremost relevant in dendroclimatological studies, i.e. when temperature reconstructions are derived. To produce a tree-ring based temperature reconstruction including low frequency variance, regional curve standardization (RCS) has to be applied (Esper et al., 2003). Thereby, the tree-ring series are aligned by cambial age and the site-specific mean growth of all age-aligned series (the so-called regional curve) is subtracted from the single series before they are dated back to calendar years. This means that the growth rates are crucial and control the level of the index series after detrending. If a regional curve from living trees of a "wrong" micro-site would be combined with subfossil material from lakes, this would result in an inappropriate detrending and biased temperature estimates (see also Düthorn et al., 2013, 2015).

In such a dendroclimatological context, micro-site differences of climate signals are also important, as the growth/climate models from living trees are transferred to the subfossil material. The growing site of the trees which fell into lakes is very likely a moist micro-site and it would thus result in a wrong climate reconstruction if the growth/climate model from the drier site would be applied. Beyond that, we found in our micro-site network that except for four locations, the temperature signals are always higher at the moist micro-site (Fig. 6). The differences of the July temperature signal are however not controlled by any analysed abiotic factor and we cannot derive any spatial pattern here, unlike for the growth rates as explained above (Fig. 5). It could be expected that trees at moister sites contain stronger temperature signals as they do not experience any water stress and can fully benefit from higher summer temperatures. However, regarding the stability of the climate signal over time, we find more often a signal decrease at moist micro-sites compared to their dry counterpart. The signal loss is generally rather small and substantial in only eight chronologies (three dry and five moist) and these are rather located in the less temperature sensitive NW and CS cluster, i.e. regions where a climate reconstruction would not be performed anyway. This means that we do not see evidence for a consistent and/or micro-site dependent divergence phenomenon as also reported by Büntgen et al. (2011).

4.4. Implications for tree-ring based temperature reconstructions in Fennoscandia

Beyond the micro-site differences and based on our network analysis, we can give an explicit recommendation for sampling locations for dendroclimatic studies aiming in the development of a summer temperature reconstruction. The NE cluster is predestined for an unbiased temperature reconstruction as we find significant July temperature signals in all chronologies (except of Ket.d), the correlation coefficients are high and largely independent to other abiotic factors including longitude or elevation. We found the highest climate signals in regions with July temperatures of 11.5–13.5 °C and May precipitation <100 mm (note that this refers to 1961–1990 mean). In that NE cluster, the moist micro-site chronologies always show a higher climate response which is ideal for merging the living tree data with subfossil material to reach millennial-length chronologies and reconstructions as described above. Regarding the climate signal stability over time, we either have +/- no changes or at most sites even a signal increase. At only one site (Kuu) the dry micro-site chronology has a higher July temperature signal and this location is the only one in that cluster where we find a substantial signal decrease over time. In general, Kuu behaves a little bit differently and shows for example the lowest correlation with the other chronologies in that cluster (Fig. 2) and can thus rather be seen as an outlier. We also have to mention that the moist chronology from that location is shorter than all the other chronologies. In all the other clusters we either have a lower climate signal and/or a strong spread of the behaviour regarding signal difference between moist and dry sites and stronger climate signal loss as already mentioned above. Another beneficial aspect for using trees from the NE cluster for a temperature reconstruction is that we also have strongest inter-chronology correlations in the cluster meaning that one could collect samples from a wider region in Fennoscandia to get the best trans-regional signal and to reduce noise from individual site factors as disturbance or alike. This finally would again result in a more robust signal assessment and subsequently temperature reconstruction.

5. Conclusion

Our Fennoscandian micro-site network reveals a general dependency of pine growth rates on latitude and July temperature. However, according to the geographical environmental conditions of Fennoscandia the network clusters into three different groups: coastal settings in the luv of the Scands in northern Norway, continental sites in the lee of the Scands north of the polar circle, and locations south of the polar circle. Differences between moist and dry sites are likely caused by associated effects on soil temperature within the respective geographical region. While trees at moist micro-sites at western locations exhibit higher growth rates, this pattern inverses under the more continental conditions of the east, where increased ring widths are found at drier sites. Next to the latitudinal increase of July temperature signals, pines at moist sites generally tend to show a higher dependency to summer warmth. The highest temperature sensitivity and growth coherency is found in those regions where July temperatures range between 11.5 and 13.5 °C and May precipitation totals fall below 100 mm, making this environment to an ideal region for a sampling aiming in a robust tree-ring based climate reconstruction.

Funding

CH and JE were supported by the German Research Foundation

[grant numbers HA 8048/1-1, Inst 247/665-1 FUGG, ES 161/9-1]. ET was partially supported by NSF-PIRE [grant number OISE-1743738] and NSF-P2C2 [grant number AGS-1702439].

Data availability

The tree-ring width data is available at the International Tree-Ring Data Bank (ITRDB).

Declaration of Competing Interest

The authors declare that they have no conflict of interest.

Acknowledgements

We are grateful to the involved municipalities and forestry administrations for sampling permissions. We thank Oli Konter, Lea Schneider, Maria Mischel, Simon Gläser, Johannes Neumann, Tineke Rook, Diana Rösch and Philipp Schön for help in the field and laboratory.

Appendix A. Supplementary data

Supplementary material related to this article can be found, in the online version, at doi:https://doi.org/10.1016/j.dendro.2020.125787.

References

Bunn, A.G., Korpela, M., Biondi, F., Mérian, P., Qeadan, F., Zang, C., 2012. dplR: Dendrochronology Program Library in R.

Büntgen, U., Raible, C.C., Frank, D., Helama, S., Cunningham, L., Hofer, D., Nievergelt, D., Verstege, A., Timonen, M., Stenseth, N.C., Esper, J., Kurths, J., 2011. Causes and consequences of past and projected scandinavian summer temperatures, 500–2100 AD. PLoS One 6, e25133. https://doi.org/10.1371/journal.pone.0025133.

Cook, E.R., Peters, K., 1981. The smoothing spline: a new approach to standardizing forest interior tree-ring width series for dendroclimatic studies. Tree-Ring Bull. 41, 45–55.

Cornes, R.C., van der Schrier, G., van den Besselaar, E.J.M., Jones, P.D., 2018. An ensemble version of the E-OBS temperature and precipitation data sets. J. Geophys. Res. Atmos. 123, 9391–9409. https://doi.org/10.1029/2017JD028200.

D'Arrigo, R.D., Wilson, R.J.S., Liepert, B., Cherubini, P., 2008. On the 'Divergence Problem' in Northern Forests: a review of the tree-ring evidence and possible causes. Glob. Planet. Change 60, 289–305. https://doi.org/10.1016/j.gloplacha.2007.03.004.

Düthorn, E., Holzkämper, S., Timonen, M., Esper, J., 2013. Influence of micro-site conditions on tree-ring climate signals and trends in central and northern Sweden. Trees – Struct. Funct. 27, 1395–1404. https://doi.org/10.1007/s00468-013-0887-8.

Düthorn, E., Schneider, L., Konter, O., Schön, P., Timonen, M., Esper, J., 2015. On the hidden significance of differing micro-sites on tree-ring based climate reconstructions. Silva Fenn. 49 https://doi.org/10.14214/sf.1220.

Düthorn, E., Schneider, L., Günther, B., Gläser, S., Esper, J., 2016. Ecological and climatological signals in tree-ring width and density chronologies along a latitudinal boreal transect. Scand. J. For. Res. 31, 750–757. https://doi.org/10.1080/02827581.2016.1181201.

Edvardsson, J., Rimkus, E., Corona, C., Šimanauskienė, R., Kažys, J., Stoffel, M., 2015. Exploring the impact of regional climate and local hydrology on Pinus sylvestris L. Growth variability – a comparison between pine populations growing on peat soils and mineral soils in Lithuania. Plant Soil 392, 345–356. https://doi.org/10.1007/s11104-015-2466-9.

Esper, J., Frank, D., 2009. Divergence pitfalls in tree-ring research. Clim. Change 94, 261–266. https://doi.org/10.1007/s10584-009-9594-2.

Esper, J., Cook, E.R., Krusic, P.J., Peters, K., 2003. Tests of the RCS method for preserving low-frequency variability in long tree-ring chronologies. Tree. Res. 59, 81–98.

Esper, J., Büntgen, U., Timonen, M., Frank, D., 2012a. Variability and extremes of northern Scandinavian summer temperatures over the past two millennia. Glob. Planet. Change 88–89, 1–9. https://doi.org/10.1016/j.gloplacha.2012.01.006.

Esper, J., Frank, D., Timonen, M., Zorita, E., Wilson, R.J.S., Luterbacher, J., Holzkämper, S., Fischer, N., Wagner, S., Nievergelt, D., Verstege, A., Büntgen, U., 2012b. Orbital forcing of tree-ring data. Nat. Clim. Chang. 2, 862–866. https://doi.org/10.1038/nclimate1589.

Esper, J., Düthorn, E., Krusic, P.J., Timonen, M., Büntgen, U., 2014. Northern European summer temperature variations over the Common Era from integrated tree-ring density records: Northern European common era summer temperatures. J. Quat. Sci. 29, 487–494. https://doi.org/10.1002/jqs.2726.

Grudd, H., 2008. Torneträsk tree-ring width and density ad 500–2004: a test of climatic sensitivity and a new 1500-year reconstruction of north Fennoscandian summers. Clim. Dyn. 31, 843–857. https://doi.org/10.1007/s00382-007-0358-2.

Gunnarson, B.E., 2001. Lake Level Changes Indicated by Dendrochronology on Subfossil Pine, Jämtland, Central Scandinavian Mountains, Sweden. Arct. Antarct. Alp. Res. 33, 274–281. https://doi.org/10.1080/15230430.2001.12003431.

Hartl, C., St. George, S., Konter, O., Harr, L., Scholz, D., Kirchhefer, A., Esper, J., 2019. Warfare dendrochronology: trees witness the deployment of the German battleship Tirpitz in Norway. Anthropocene 27, 100212. https://doi.org/10.1016/j.ancene.2019.100212.

Hartl-Meier, C., Dittmar, C., Zang, C., Rothe, A., 2014. Mountain forest growth response to climate change in the Northern Limestone Alps. Trees – Struct. Funct. 28, 819–829. https://doi.org/10.1007/s00468-014-0994-1.

Helama, S., Mielikäinen, K., Timonen, M., Eronen, M., 2008. Finnish supra-long tree-ring chronology extended to 5634 BC. Nor. Geogr. Tidsskr. 62, 271–277. https://doi.org/10.1080/00291950802517593.

Hellmann, L., Agafonov, L., Ljungqvist, F.C., Churakova Sidorova, O., Düthorn, E., Esper, J., Hülsmann, L., Kirdyanov, A.V., Moiseev, P., Myglan, V.S., Nikolaev, A.N., Reinig, F., Schweingruber, F.H., Solomina, O., Tegel, W., Büntgen, U., 2016. Diverse growth trends and climate responses across Eurasia's boreal forest. Environ. Res. Lett. 11, 074021. https://doi.org/10.1088/1748-9326/11/7/074021.

Holmes, R.L., 1983. Computer-assisted quality control in tree-ring dating and measurement. Tree-Ring Bull. 43, 69–78.

Körner, C., 2012. Alpine Treelines: Functional Ecology of the Global High Elevation Tree Limits. Springer, Basel [u.a.].

Lange, J., Buras, A., Cruz-García, R., Gurskaya, M., Jalkanen, R., Kukarskih, V., Seo, J.-W., Wilmking, M., 2018. Climate regimes override micro-site effects on the summer temperature signal of scots pine at its northern distribution limits. Front. Plant Sci. 9, 1597. https://doi.org/10.3389/fpls.2018.01597.

Linderholm, H., 2001. Climatic influence on Scots pine growth on dry and wet soils in the central Scandinavian mountains, interpreted from tree-ring width. Silva Fenn. 35 https://doi.org/10.14214/sf.574.

Linderholm, H.W., Gunnarson, B.E., 2005. Summer temperature variability in central Scandinavia during the last 3600 years. Geogr. Ann. Ser. A Phys. Geogr. 87, 231–241. https://doi.org/10.1111/j.0435-3676.2005.00255.x.

Linderholm, H.W., Moberg, A., Grudd, H., 2002. Peatland pines as climate indicators? A regional comparison of the climatic influence on Scots pine growth in Sweden. Can. J. For. Res. 32, 1400–1410. https://doi.org/10.1139/x02-071.

Linderholm, H.W., Björklund, J.A., Seftigen, K., Gunnarson, B.E., Grudd, H., Jeong, J.-H., Drobyshev, I., Liu, Y., 2010. Dendroclimatology in Fennoscandia – from past accomplishments to future potential. Clim. Past Discuss. 6, 93–114. https://doi.org/10.5194/cp-6-93-2010.

Linderholm, H.W., Zhang, P., Gunnarson, B.E., Björklund, J., Farahat, E., Fuentes, M., Rocha, E., Salo, R., Seftigen, K., Stridbeck, P., Liu, Y., 2014. Growth dynamics of tree-line and lake-shore Scots pine (Pinus sylvestris L.) in the central Scandinavian Mountains during the Medieval Climate Anomaly and the early Little Ice Age. Front. Ecol. Evol. 2 https://doi.org/10.3389/fevo.2014.00020.

Loader, N.J., Young, G.H.F., Grudd, H., McCarroll, D., 2013. Stable carbon isotopes from Torneträsk, northern Sweden provide a millennial length reconstruction of summer sunshine and its relationship to Arctic circulation. Quat. Sci. Rev. 62, 97–113. https://doi.org/10.1016/j.quascirev.2012.11.014.

Matskovsky, V.V., Helama, S., 2014. Testing long-term summer temperature reconstruction based on maximum density chronologies obtained by reanalysis of tree-ring data sets from northernmost Sweden and Finland. Clim. Past Discuss. 10, 1473–1487. https://doi.org/10.5194/cp-10-1473-2014.

McCarroll, D., Loader, N.J., Jalkanen, R., Gagen, M.H., Grudd, H., Gunnarson, B.E., Kirchhefer, A.J., Friedrich, M., Linderholm, H.W., Lindholm, M., Boettger, T., Los, S. O., Remmele, S., Kononov, Y.M., Yamazaki, Y.H., Young, G.H., Zorita, E., 2013. A 1200-year multiproxy record of tree growth and summer temperature at the northern pine forest limit of Europe. Holocene 23, 471–484. https://doi.org/10.1177/0959683612467483.

Mosteller, F., Tukey, J.W., 1977. Data Analysis and Regression: a Second Course in Statistics, Addison-wesley Series in Behavioral Science. Quantitative Methods. Addison-Wesley Pub. Co., Reading; Mass.

Paulsen, J., Weber, U.M., Körner, C., 2000. Tree growth near Treeline: abrupt or gradual reduction with altitude? Arct. Antarct. Alp. Res. 32, 14–20.

Wilmking, M., D'Arrigo, R., Jacoby, G.C., Juday, G.P., 2005. Increased temperature sensitivity and divergent growth trends in circumpolar boreal forests. Geophys. Res. Lett. 32, L15715. https://doi.org/10.1029/2005GL023331.

Wilmking, van der Maaten-Theunissen, M., van der Maaten, E., Scharnweber, T., Buras, A., Biermann, C., Gurskaya, M., Hallinger, M., Lange, J., Shetti, R., Smiljanic, M., Trouillier, M., 2020. Global assessment of relationships between climate and tree growth. Glob Change Biol gcb. 15057 https://doi.org/10.1111/gcb.15057.

Wood, S.N., 2017. Generalized Additive Models : an Introduction With R. Chapman and Hall/CRC. https://doi.org/10.1201/9781315370279.

Young, G.H.F., McCarroll, D., Loader, N.J., Gagen, M.H., Kirchhefer, A.J., Demmler, J.C., 2012. Changes in atmospheric circulation and the Arctic Oscillation preserved within a millennial length reconstruction of summer cloud cover from northern Fennoscandia. Clim. Dyn. 39, 495–507. https://doi.org/10.1007/s00382-011-1246-3.

Zang, C., Biondi, F., 2015. Treeclim: an R package for the numerical calibration of proxy-climate relationships. Ecography 38, 431–436. https://doi.org/10.1111/ecog.01335.